MOF Membranes

International Edition: DOI: 10.1002/anie.201810925
German Edition: DOI: 10.1002/ange.201810925

Incorporation of Homochirality into a Zeolitic Imidazolate Framework Membrane for Efficient Chiral Separation

Jun Yong Chan, Huacheng Zhang, Yada Nolvachai, Yaoxin Hu, Haijin Zhu, Maria Forsyth, Qinfen Gu, David E. Hoke, Xiwang Zhang, Philip J. Marriot, and Huanting Wang**

Abstract: *Homochiral metal–organic frameworks (MOFs) have gained much attention because of their chiral properties and disposition for chiral separation. However, the fabrication of high-quality homochiral MOF membranes remains challenging because of the difficulty in controlling growth of MOF membranes with chiral functionalities. A homochiral zeolitic imidazolate framework-8 (ZIF-8) membrane is reported for efficient chiral separation. The membrane is synthesized by incorporating a natural amino acid,* L*-histidine (*L*-His), into the framework of ZIF-8. The homochiral* L*-His-ZIF-8 membrane exhibits a good selectivity for the R-enantiomer of 1-phenylethanol over the S-enantiomer, showing a high enantiomeric excess value up to 76%.*

Chirality is a unique property of molecular isomers that manifests as non-superposition of the mirror images of those isomers. This property plays an essential role in aspects of medical and life sciences, food chemistry, and drug manufacture.[1] With intrinsic biological effects/activities that are highly specific to each enantiomer, considerable research efforts have been directed toward developing advanced techniques that allow discrimination between chiral compounds; including, spontaneous crystallization, enzymatic kinetic resolution, and the use of enantioselective stationary phases in chromatography.[2] In the last decade, metal–organic frameworks (MOFs) and their derivative membranes have emerged as promising materials for molecular separation as these exhibit pores of defined and tunable dimensions, with high surface area, and generally good adsorption properties.[3] While the main research focus has been on the applications of MOFs for processes such as gas storage, gas separation, catalytic processes and drug delivery,[4] a few new MOF materials with chiral properties have been reported recently that are capable of chiral separation. Conceptually, homochiral MOFs with a chiral environment in the open channels of the framework may be synthesized in the following ways: 1) directly, using a chiral (enantiopure) ligand;[5] 2) through formation of secondary building units with a chiral linker;[6] 3) by post synthesis of achiral MOF;[7] or 4) by self-assembly of chiral ligands.[8] The self-assembled chiral ligands can sometimes be complex and expensive, but in none of these cases can success be guaranteed.

In addition to separation based on MOF particles/columns, membrane-based separations show potential advantages over other techniques because of their low operating cost, low energy consumption, and potential for scalability.[9] However, MOF membranes are still relatively new to the chiral separations field, and thus reports of homochiral MOF membranes are relatively limited to date. For instance, Wang et al. reported the successful fabrication of [Zn_2(bdc)-(L-lac)(dmf)] (1,4-benzenedicarboxylic acid (bdc), L-lactate (L-lac), dimethylformamide (dmf)) membrane, which achieved an enantiomeric excess (*ee*%) value of 33% with *R*-methyl phenyl sulfoxide in excess.[10] Another homochiral MOF [Ni_2(L-asp)(bipy)] (L-aspartic acid (L-asp), 2,2′-bipyridine (bipy)) membrane was reported by the same group that was able to separate racemic 2-methyl-2,4-pentadiol with an *ee*% of 35.5 ± 2.5% (*R*-enantiomer in excess).[10] These works demonstrate the potential of homochiral MOF membranes in chiral separation, but the selectivity of MOF membranes remain relatively low. Therefore, it is important to fabricate MOF membranes with high chiral selectivity.

Herein, we report a homochiral zeolitic imidazolate framework, L-His-ZIF-8 (Zn(Hmim/L-His)$_2$: 2-methylimidazolate (Hmim), L-histidine (L-His)), membrane to efficiently separate racemic 1-phenylethanol, the *R*-enantiomer of which is a useful chemical as ophthalmic preservative, inhibitor of cholesterol adsorption, and component of fragrances.[11] The homochiral L-His-ZIF-8 membrane is synthesized by incorporating a natural amino acid, L-His, into the ZIF-8 framework using a contra diffusion method.[12] The L-His-ZIF-8 membrane showed good capability in separating the *R*- and *S*-enantiomer of racemic 1-phenylethanol, thereby allowing preferential permeation of the *R*-enantiomer across the membrane with an enantiomeric excess value up to 76% with *R*-(+)-1-phenylethanol in excess. Such a high chiral

[*] J. Y. Chan, Dr. H. Zhang, Dr. Y. Hu, Prof. X. Zhang, Prof. H. Wang
Department of Chemical Engineering, Monash University
Clayton, Victoria 3800 (Australia)
E-mail: huacheng.zhang@monash.edu
huanting.wang@monash.edu
Y. Nolvachai, Prof. P. J. Marriot
Australian Centre for Research on Separation Science
Department of Chemistry, Monash University
Clayton, Victoria 3800 (Australia)
Dr. H. Zhu, Prof. M. Forsyth
Institute for Frontier Materials, Deakin University
Geelong Victoria 3216 (Australia)
Dr. Q. Gu
Australian Synchrotron
800 Blackburn Rd, Clayton Victoria 3168 (Australia)
D. E. Hoke
Department of Biochemistry and Molecular Biology
Monash University
Clayton, Victoria 3800 (Australia)
Supporting information and the ORCID identification number(s) for the author(s) of this article can be found under: https://doi.org/10.1002/anie.201810925.

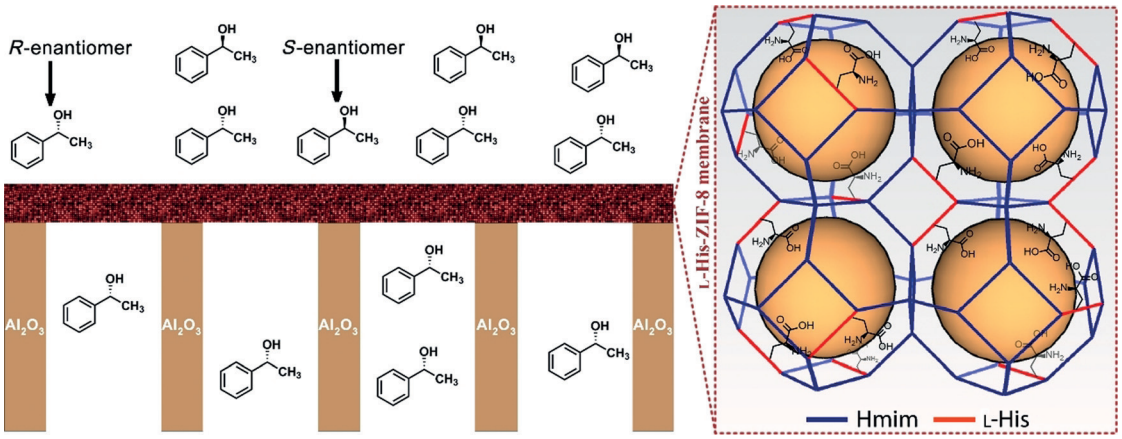

Figure 1. A representation of a homochiral L-His-ZIF-8-membrane for separating the *R*-enantiomer of 1-phenylethanol from the *S*-enantiomer.

selectivity of the L-His-ZIF-8 membrane is attributed to the specific interaction between the *S*-enantiomer and the chiral MOF framework.

As shown schematically in Figure 1, a chiral selector layer of L-His-ZIF-8 was grown on a 20 nm porous anodic aluminum oxide (AAO) support (Supporting Information, Figure S1) by an in situ growth method (Supporting Information, Experimental Section). The existence of L-His introduced a homochiral environment in the framework and allowed *R*-(+)-1-phenylethanol to pass through. The membrane morphology was determined with scanning electron microscopy (SEM). Top-view SEM images reveal a continuous film of L-His-ZIF-8 with good intergrowth, which suggests that the membrane possesses high integrity (Figure 2a). A magnified image showed that L-His-ZIF-8 covers the AAO substrate fully (Figure 2b). The integrity of the L-His-ZIF-8 membrane was further examined with gas permeation experiments, which suggest excellent gas selectivities and high membrane quality (Figure S2). From the cross-sectional view (Figure 2c), a consistent layer of L-His-ZIF-8 with a thickness of approximately 3.9 ± 0.19 μm was obtained. To further examine the quality of the L-His-ZIF-8 layer grown on the porous AAO support, the crystal structures of both L-His-ZIF-8 crystal and membrane were examined. According to the X-ray diffraction (XRD) pattern (Figure 2e), L-His-ZIF-8 showed a similar crystal structure to that of ZIF-8 with no extra XRD peaks. Typical characteristic peaks of ZIF-8 with 2θ at 7.4°, 10.4°, and 12.8° were observed with slight shifts to larger angles—indicating that L-His-ZIF-8 exhibits the same sodalite (SOD) topology as ZIF-8 with a slightly smaller unit cell. The peak shift was caused by the incorporation of the amino acid L-His, which causes slight lattice distortion in the crystal according to previous studies.[13] On the other hand, the chirality in MOF crystals exerts lattice distortions because homochiral amino acid is present, and therefore the incorporation of L-his can be further justified.[14]

To prove the successful incorporation of L-His into the L-His-ZIF-8 framework, the L-His-ZIF-8 ($Zn(Hmim/L\text{-}His)_2$) and ZIF-8 ($Zn(Hmim)_2$) membranes/crystals were systematically characterized with element mapping by energy-dispersive X-ray spectroscopy (EDX), Fourier-transform infrared (FTIR) spectroscopy, X-ray photoelectron spectroscopy (XPS), and solid-state nuclear magnetic resonance (NMR). With respect to the molecular structures of the Hmim and L-His organic ligands, L-His comprises additional amine groups ($-NH_2$) and carboxy groups (-COOH) compared to Hmim, which allows its presence in the framework of L-His-ZIF-8 to be identified. As shown in Figure 2d, the elemental mapping of the cross-section of the L-His-ZIF-8/AAO membrane showed a sufficient amount of oxygen atoms on the L-His-ZIF-8 layer, corresponding to the two additional oxygen atoms of the carboxy group in the L-his molecular

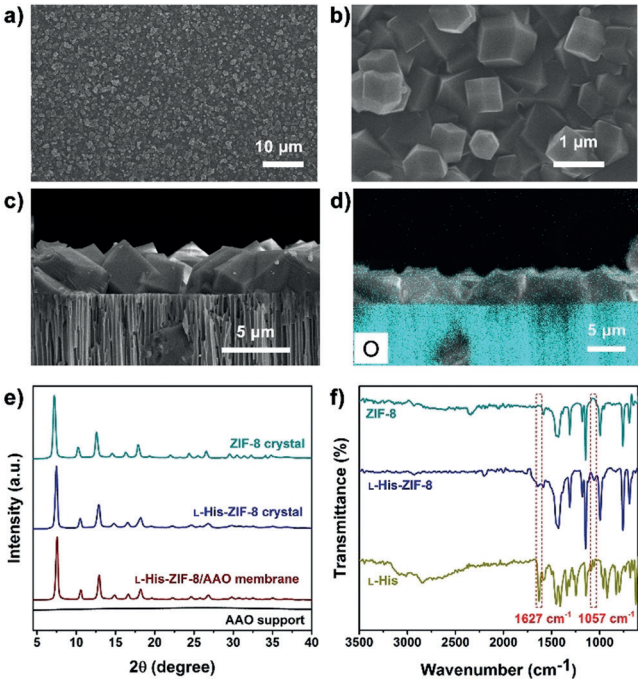

Figure 2. a,b) SEM images of the top surface of L-His-ZIF-8/AAO membrane at low (a) and high (b) magnifications. c) SEM image of the cross-section of the membrane. d) XRD patterns of ZIF-8 crystal, L-His-ZIF-8 crystal, L-His-ZIF-8 crystal/AAO membrane, and AAO support. e) EDX elemental mapping of oxygen on the cross-section of the L-His-ZIF-8/AAO membrane. f) FTIR spectra of L-His-ZIF-8, ZIF-8, and L-His. Insets indicate the chemical molecular structures of L-His-ZIF-8, ZIF-8, and L-His, respectively.

structure. As a comparison, elemental mapping of the ZIF-8/AAO membrane confirmed that the oxygen atoms did not exist in the ZIF-8 layer (Figure S3). FTIR spectroscopy of L-His presents an adsorption peak at 1627 cm^{-1}; this was attributed to the C=O stretch in the carboxy group for L-His, which was observed to have a slight shift to 1648 cm^{-1} for L-His-ZIF-8 (Figure 2 f). An additional adsorption peak was also found at 1057 cm^{-1} in L-His and L-His-ZIF-8, which corresponded to the side-chain amine group of L-His. However, FTIR spectroscopy of ZIF-8 did not present these two adsorption peaks. Analysis of the C 1s spectrum by XPS identified the binding energy of the carboxylic group (-COOH) of L-His-ZIF-8 at 288.21 eV; this peak was not present in ZIF-8[15] (Figure S4). A comparison of the O 1s spectra of L-His-ZIF-8 and ZIF-8 revealed a larger signal at 531.3 eV for L-His-ZIF-8 (Tables S1 and S2). On the basis of the atomic percentage (at%) of L-His-ZIF-8, the ratio of L-His to Hmim is calculated to be 1:9. Solid-state NMR was performed to further verify the incorporation of L-His into the framework. Additional peaks attributed to L-his were identified compared to pure ZIF-8 with several peak shifts. Peak shifts corresponding to L-His arise because of the bonding of L-His within the framework (Figure S5).

Circular dichroism (CD) spectroscopy and nitrogen sorption isotherm measurements were performed to confirm the chirality and porosity of the L-His-ZIF-8 membrane. Compared with pure ZIF-8, there is an adsorption peak at 234 cm^{-1} in the CD spectrum of the L-His-ZIF-8 membrane that demonstrates its homochirality (Figure S6). Furthermore, nitrogen adsorption analysis results showed that the Brunauer–Emmett–Teller (BET) surface area of L-His-ZIF-8 was 1275.9 $m^2 g^{-1}$ with a micropore volume of 0.34 $cm^3 g^{-1}$ (Figure S7), indicating that L-His-ZIF-8 possessed a typical porous structure with a high surface area.

High-quality L-His-ZIF-8/AAO membrane was used to separate enantiomers of 1-phenylethanol. Since the enantioselectivities of a homochiral MOF arise from the chiral environment in open channels,[16] one of the enantiomers is expected to interact with the chiral L-His-ZIF-8 framework and pass through the membrane at a slower rate than the other enantiomer. The separation process was performed in a homemade diffusion cell and the concentration gradient was used as the driving force. Real-time components of the permeate solution were analyzed every 2 h by enantioselective gas chromatography (GC) analysis.

Single-component permeation experiments were performed to evaluate the diffusion flux of *R*-(+)-1-phenylethanol and *S*-(−)-1-phenylethanol. The elution times of the *R*- and *S*-enantiomers were identified at around 6.03 min and 6.42 min, respectively. As shown in Figure S8, *R*-(+)-1-phenylethanol diffusion through the membrane is much faster than *S*-(−)-1-phenylethanol. *R*-(+)-1-phenylethanol flux is 1.87×10^{-6} mol $m^{-2} s^{-1}$ and *S*-(−)-1-phenylethanol flux is 0.19×10^{-6} mol $m^{-2} s^{-1}$, and thus, the ideal selectivity of *R*-(+)-1-phenylethanol over *S*-(−)-1-phenylethanol is 9.5. A mixture of *R*-(+)-1-phenylethanol and *S*-(−)-1-phenylethanol (50:50) was then used to determine the separation property of the L-His-ZIF-8 membrane. Figure 3 shows the GC results of the permeate solution versus time, where different intensities

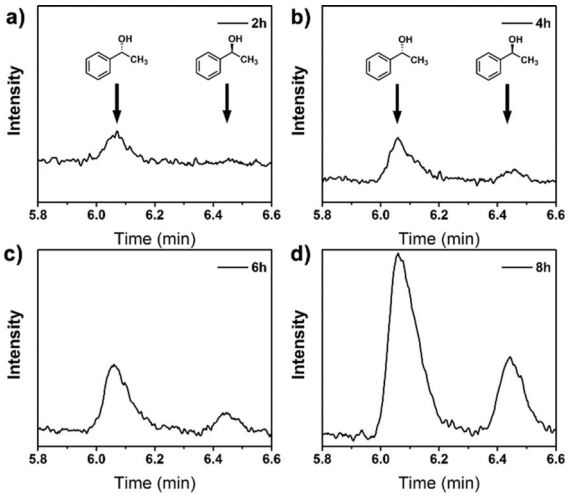

Figure 3. Gas chromatograms of resolved 1-phenylethanol enantiomers after separation for a) 2 h, b) 4 h, c) 6 h, and d) 8 h under conditions of 0.008 mol L^{-1} feed solution at room temperature.

of enantiomer peaks were observed. The GC results provided the most direct evidence that L-His-ZIF-8 was capable of performing chiral separation. The different peak areas of both enantiomers were obvious in the corresponding GC chromatograms (Figure 3; Figures S9 and S10) and *R*-(+)-1-phenylethanol generally showed greater peak response compared to *S*-(−)-1-phenylethanol. Compared with pure ZIF-8 membrane (Figure S11), no differences in peak areas were observed, indicating the achiral ZIF-8 is not capable of performing chiral separation. Note that there is no peak of *S*-(−)-1-phenylethanol detected when the permeation time is shorter than 2 h. Therefore, all permeation data presented in this work starts at 2 h. Figure 4 a shows the enantioselectivity of the membrane when 0.008 mol L^{-1} racemic 1-phenylethanol in feed solution was measured in the receiving solution side of the membrane over 8 h measurements. The highest enantiomeric excess (*ee*%) of 76% was observed in the first 2 h with the *R*-enantiomer in excess. As shown in Figure 4 b, the membrane showed an *R*-(+)-1-phenylethanol flux of 1.42×10^{-6} mol $m^{-2} s^{-1}$ and *S*-(−)-1-phenylethanol flux of 0.193×10^{-6} mol $m^{-2} L^{-1}$ in the first 2 h. The mixed selectivity of R-(+)-1-phenylethanol over S-(−)-1-phenylethanol is 7.34, which is lower than the ideal selectivity, as expected. As the diffusion proceeded, the diffusion rates of both

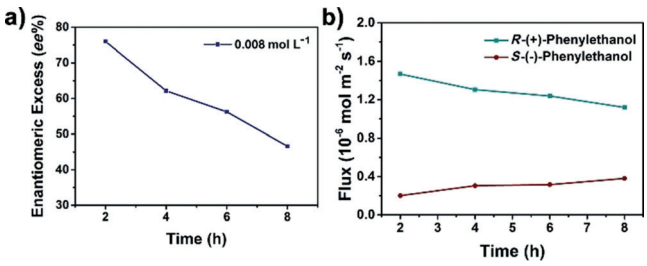

Figure 4. Chiral separation results under conditions of 0.008 mol L^{-1} racemic 1-phenylethanol as a feed solution at room temperature. a) Enantiomeric excess (*ee*%) and b) concentration of each enantiomer at the permeate side as a function of time.

enantiomers decreased but the concentration of *R*-(+)-1-phenylethanol still remained higher than that of *S*-(−)-1-phenylethanol, suggesting L-His-ZIF-8 has higher affinity to interact with *S*-(−)-1-phenylethanol. During the permeation process, the feed concentrations decreased and the permeate concentrations decreased with time (Figure S12), leading to a reduction in concentration gradients. As shown in Figure 4b, *R*-(+)-1-phenylethanol flux decreases with permeation time, whereas S-(−)-1-phenylethanol flux increases slightly because the permeation tends to reach equilibrium.[17] These two factors contribute to a gradual decrease in *ee*%, with 46.6% at 8 h.

To investigate the effect of feed concentration, 0.004 mol L^{-1} and 0.006 mol L^{-1} racemic 1-phenylethanol concentrations were used in feed solutions (Figures S13 and S14). The results showed a similar *ee*% and the same declining trend in *ee*% with an increase in permeation time.

To understand the chiral separation mechanisms in the L-His-ZIF-8 membrane, we performed high-resolution synchrotron powder XRD (PXRD) and solid-state NMR experiments to identify permeation pathways. The lattice parameters of L-His-ZIF-8 calculated from the synchrotron PXRD data before and after the permeation experiments are compared in Table S3. A 3D framework distortion of L-His-ZIF-8 unit cells after the permeation was observed, suggesting that the chiral molecules do indeed enter into the framework. Meanwhile, the solid-state NMR analysis of L-His-ZIF-8 after the permeation showed two peak shifts at about 14 ppm and 124 ppm, while the other peaks remained at the same positions; these results suggest that the interaction of chiral molecules and L-His-ZIF-8 is spatially close to these two sites at a molecular level (Figure S15). Therefore, *S*-phenylethanol is more easily adsorbed in the chiral channel of L-His-ZIF-8 while *R*-phenylethanol preferentially passes through the membrane.

To prove the reproducibility of the membrane preparation, we also performed the above chiral separations using three membranes and the average *ee*% is shown in Figure S16. Consistent *ee*% values ranging from 56% to 60% were observed in the first sampling analysis, which reduced to 27% to 28% in the final analysis. Therefore, the concentration of feed solution did not have a significant impact on the chiral selectivity. Furthermore, we examined the effect of AAO support by using it for separation under the same conditions. The results show that AAO support does not have any chiral selectivity, and thus the effect of support on chiral selectivity is negligible.

In addition to excellent chiral separation performance, the L-His-ZIF-8 membrane exhibits good stability. Firstly, ZIF-8 was previously reported to be stable in ethanol—the diffusion medium used in this work.[18] Moreover, experimental data has proven the consistency of enantioselectivity over three separations of racemic 1-phenylethanol with different concentrations. The SEM and XRD results demonstrate the integrity of the membrane after the tests. Figures 5a and b show that the L-His-ZIF-8 crystals remained intact on the support even after three cycles of separation. The XRD patterns confirmed that the crystal structure of the membrane remained the same (Figure 5c).

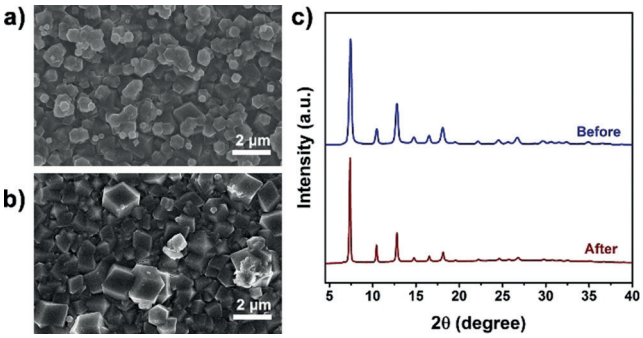

Figure 5. SEM images of the L-His-ZIF-8/AAO membrane a) before and b) after tests. c) XRD patterns of the L-His-ZIF-8/AAO membrane before and after tests.

In summary, we have successfully incorporated homochiral amino acid L-His into a ZIF-8 membrane; namely, a L-His-ZIF-8 membrane. The chiral environment in this framework made it the first chiral ZIF membrane capable of chiral separation. In particular, the AAO supported membrane is prepared with a continuous L-His-ZIF-8 layer of approximately 3.9 μm thickness. The L-His-ZIF-8 membrane exhibits good chiral selectivity for racemic 1-phenylethanol. The highest *ee*% of 76% with *R*-(+)-1-phenylethanol in excess was achieved for a feed concentration of 0.008 mol L^{-1} at room temperature. Moreover, the membrane did not show any loss in enantioselectivity after three cycles of separation. This work provides a new insight into the preparation of homochiral MOF membranes with high selectivity for potential practical chiral separation.

Acknowledgements

This research is supported by the Australian Research Council (DP170102964 and DE170100006). This work was performed, in part, at the Victorian node of the Australian National Fabrication Facility—a company established under the National Collaborative Research Infrastructure Strategy to provide nano- and microfabrication facilities for Australia's researchers. Deakin University's Advanced Facility is acknowledged for use of the NMR instrument. Part of the experiment was performed at the powder diffraction beamline, Australian Synchrotron (ANSTO).

Conflict of interest

The authors declare no conflict of interest.

Keywords: chiral resolution · chirality · homochiral · membrane separation · metal–organic frameworks

How to cite: *Angew. Chem. Int. Ed.* **2018**, *57*, 17130–17134
Angew. Chem. **2018**, *130*, 17376–17380

[1] a) I. Ilisz, A. Péter, W. Lindner, *TrAC Trends Anal. Chem.* **2016**, *81*, 11–22; b) G. K. E. Scriba in *Chiral Separations: Methods and*

Protocols (Ed.: G. K. E. Scriba), Humana Press, Totowa, **2013**, pp. 1 – 27.
[2] a) F. Faigl, E. Fogassy, M. Nógrádi, E. Pálovics, J. Schindler, *Tetrahedron: Asymmetry* **2008**, *19*, 519 – 536; b) Q. Wu, Y. Sun, J. Gao, S. Dong, G. Luo, H. Li, L. Zhao, *TrAC Trends Anal. Chem.* **2017**, *86*, 25; c) N. M. Maier, P. Franco, W. Lindner, *J. Chromatogr. A* **2001**, *906*, 3 – 33.
[3] a) S. Qiu, M. Xue, G. Zhu, *Chem. Soc. Rev.* **2014**, *43*, 6116 – 6140; b) M. Rubio-Martinez, C. Avci-Camur, A. W. Thornton, I. Imaz, D. Maspoch, M. R. Hill, *Chem. Soc. Rev.* **2017**, *46*, 3453 – 3480; c) H. Li, M. Eddaoudi, M. O'Keeffe, O. M. Yaghi, *Nature* **1999**, *402*, 276 – 279; d) G. Nickerl, A. Henschel, R. Grünker, K. Gedrich, S. Kaskel, *Chem. Ing. Tech.* **2011**, *83*, 90 – 103.
[4] a) J.-R. Li, J. Sculley, H.-C. Zhou, *Chem. Rev.* **2012**, *112*, 869 – 932; b) J.-R. Li, R. J. Kuppler, H.-C. Zhou, *Chem. Soc. Rev.* **2009**, *38*, 1477 – 1504; c) J. Lee, O. K. Farha, J. Roberts, K. A. Scheidt, S. T. Nguyen, J. T. Hupp, *Chem. Soc. Rev.* **2009**, *38*, 1450 – 1459; d) T.-H. Bae, J. S. Lee, W. Qiu, W. J. Koros, C. W. Jones, S. Nair, *Angew. Chem. Int. Ed.* **2010**, *49*, 9863 – 9866; *Angew. Chem.* **2010**, *122*, 10059 – 10062; e) P. Horcajada, T. Chalati, C. Serre, B. Gillet, C. Sebrie, T. Baati, J. F. Eubank, D. Heurtaux, P. Clayette, C. Kreuz, J. S. Chang, Y. K. Hwang, V. Marsaud, P. N. Bories, L. Cynober, S. Gil, G. Ferey, P. Couvreur, R. Gref, *Nat. Mater.* **2010**, *9*, 172 – 178; f) C.-Y. Sun, C. Qin, C.-G. Wang, Z.-M. Su, S. Wang, X.-L. Wang, G.-S. Yang, K.-Z. Shao, Y.-Q. Lan, E.-B. Wang, *Adv. Mater.* **2011**, *23*, 5629 – 5632; g) J. Yao, H. Wang, *Chem. Soc. Rev.* **2014**, *43*, 4470 – 4493; h) Y. Hu, J. Wei, Y. Liang, H. Zhang, X. Zhang, W. Shen, H. Wang, *Angew. Chem. Int. Ed.* **2016**, *55*, 2048 – 2052; *Angew. Chem.* **2016**, *128*, 2088 – 2092.
[5] a) K. J. Hartlieb, J. M. Holcroft, P. Z. Moghadam, N. A. Vermeulen, M. M. Algaradah, M. S. Nassar, Y. Y. Botros, R. Q. Snurr, J. F. Stoddart, *J. Am. Chem. Soc.* **2016**, *138*, 2292 – 2301; b) Z.-G. Gu, C. Zhan, J. Zhang, X. Bu, *Chem. Soc. Rev.* **2016**, *45*, 3122 – 3144; c) J. Navarro-Sánchez, A. I. Argente-García, Y. Moliner-Martínez, D. Roca-Sanjuán, D. Antypov, P. Campíns-Falcó, M. J. Rosseinsky, C. Martí-Gastaldo, *J. Am. Chem. Soc.* **2017**, *139*, 4294 – 4297; d) M. Xue, B. Li, S. Qiu, B. Chen, *Mater. Today* **2016**, *19*, 503 – 515.
[6] a) D. N. Dybtsev, A. L. Nuzhdin, H. Chun, K. P. Bryliakov, E. P. Talsi, V. P. Fedin, K. Kim, *Angew. Chem. Int. Ed.* **2006**, *45*, 916 – 920; *Angew. Chem.* **2006**, *118*, 930 – 934; b) R. Vaidhyanathan, D. Bradshaw, J.-N. Rebilly, J. P. Barrio, J. A. Gould, N. G. Berry, M. J. Rosseinsky, *Angew. Chem. Int. Ed.* **2006**, *45*, 6495 – 6499; *Angew. Chem.* **2006**, *118*, 6645 – 6649.
[7] J. Bonnefoy, A. Legrand, E. A. Quadrelli, J. Canivet, D. Farrusseng, *J. Am. Chem. Soc.* **2015**, *137*, 9409 – 9416.
[8] a) C.-D. Wu, A. Hu, L. Zhang, W. Lin, *J. Am. Chem. Soc.* **2005**, *127*, 8940 – 8941; b) K. Wu, K. Li, Y.-J. Hou, M. Pan, L.-Y. Zhang, L. Chen, C.-Y. Su, *Nat. Commun.* **2016**, *7*, 10487; c) G. Li, W. Yu, Y. Cui, *J. Am. Chem. Soc.* **2008**, *130*, 4582 – 4583; d) L. Ma, J. M. Falkowski, C. Abney, W. Lin, *Nat. Chem.* **2010**, *2*, 838 – 846; e) T. Liu, Y. Liu, W. Xuan, Y. Cui, *Angew. Chem. Int. Ed.* **2010**, *49*, 4121 – 4124; *Angew. Chem.* **2010**, *122*, 4215 – 4218; f) G. Li, W. Yu, J. Ni, T. Liu, Y. Liu, E. Sheng, Y. Cui, *Angew. Chem. Int. Ed.* **2008**, *47*, 1245 – 1249; *Angew. Chem.* **2008**, *120*, 1265 – 1269; g) W. Xuan, M. Zhang, Y. Liu, Z. Chen, Y. Cui, *J. Am. Chem. Soc.* **2012**, *134*, 6904 – 6907; h) K. Mo, Y. Yang, Y. Cui, *J. Am. Chem. Soc.* **2014**, *136*, 1746 – 1749; i) T. Duerinck, J. F. M. Denayer, *Chem. Eng. Sci.* **2015**, *124*, 179 – 187.
[9] R. Xie, L.-Y. Chu, J.-G. Deng, *Chem. Soc. Rev.* **2008**, *37*, 1243 – 1263.
[10] a) W. Wang, X. Dong, J. Nan, W. Jin, Z. Hu, Y. Chen, J. Jiang, *Chem. Commun.* **2012**, *48*, 7022 – 7024; b) Z. Kang, M. Xue, L. Fan, J. Ding, L. Guo, L. Gao, S. Qiu, *Chem. Commun.* **2013**, *49*, 10569 – 10571; c) K. Huang, X. Dong, R. Ren, W. Jin, *AIChE J.* **2013**, *59*, 4364 – 4372.
[11] a) M. Habulin, M. Primožič, Ž. Knez in *Modern Biocatalysis: Stereoselective and Environmentally Friendly Reactions* (Eds: W.-D. Fessner, T. Anthonsen), Wiley-VCH, Weinheim, **2009**, Chapter 8; b) Y. Fan, Z. Xie, H. Zhang, J. Qian, *Kinet. Catal.* **2011**, *52*, 686.
[12] J. Yao, D. Dong, D. Li, L. He, G. Xu, H. Wang, *Chem. Commun.* **2011**, *47*, 2559 – 2561.
[13] a) S. Borukhin, L. Bloch, T. Radlauer, A. H. Hill, A. N. Fitch, B. Pokroy, *Adv. Funct. Mater.* **2012**, *22*, 4216 – 4224; b) A. Brif, L. Bloch, B. Pokroy, *CrystEngComm* **2014**, *16*, 3268 – 3273.
[14] S.-Y. Zhang, D. Li, D. Guo, H. Zhang, W. Shi, P. Cheng, L. Wojtas, M. J. Zaworotko, *J. Am. Chem. Soc.* **2015**, *137*, 15406 – 15409.
[15] J. S. Stevens, A. C. de Luca, M. Pelendritis, G. Terenghi, S. Downes, S. L. M. Schroeder, *Surf. Interface Anal.* **2013**, *45*, 1238 – 1246.
[16] a) L. Ma, C. Abney, W. Lin, *Chem. Soc. Rev.* **2009**, *38*, 1248 – 1256; b) J.-T. Yu, Y.-Y. Shi, J. Sun, J. Lin, Z.-T. Huang, Q.-Y. Zheng, *Sci. Rep.* **2013**, *3*, 2947.
[17] F. Zaera, *Chem. Soc. Rev.* **2017**, *46*, 7374 – 7398.
[18] K. Zhang, R. P. Lively, M. E. Dose, A. J. Brown, C. Zhang, J. Chung, S. Nair, W. J. Koros, R. R. Chance, *Chem. Commun.* **2013**, *49*, 3245 – 3247.

Manuscript received: September 21, 2018
Accepted manuscript online: October 29, 2018
Version of record online: November 27, 2018

